Stem cell-mediated natural tissue engineering

H. Möllmann [a, b, *, #], H.M. Nef [a, b, #], S. Voss [b, #], C. Troidl [b], M. Willmer [b], S. Szardien [a, b], A. Rolf [a], M. Klement [b], R. Voswinckel [c], S. Kostin [d], H.A. Ghofrani [c], C.W. Hamm [a], A. Elsässer [b]

[a] *Kerckhoff Heart Center, Dept. of Cardiology, Bad Nauheim, Germany*
[b] *Franz Groedel Institute of the Kerckhoff Heart Center, Experimental Cardiology, Bad Nauheim, Germany*
[c] *Kerckhoff Heart Center, Dept. of Pulmology, Bad Nauheim, Germany*
[d] *Max-Planck-Institute for Heart and Lung Research, Bad Nauheim, Germany*

Received: June 4, 2009; Accepted: November 10, 2009

Abstract

Recently, we demonstrated that a fully differentiated tissue developed on a ventricular septal occluder that had been implanted due to infarct-related septum rupture. We suggested that this tissue originated from circulating stem cells. The aim of the present study was to evaluate this hypothesis and to investigate the physiological differentiation and transdifferentiation potential of circulating stem cells. We developed an animal model in which a freely floating membrane was inserted into each the left ventricle and the descending aorta. Membranes were removed after pre-specified intervals of 3 days, and 2, 6 and 12 weeks; the newly developed tissue was evaluated using quantitative RT-PCR, immunohistochemistry and *in situ* hybridization. The contribution of stem cells was directly evaluated in another group of animals that were by treated with granulocyte macrophage colony-stimulating factor (GM-CSF) early after implantation. We demonstrated the time-dependent generation of a fully differentiated tissue composed of fibroblasts, myofibroblasts, smooth muscle cells, endothelial cells and new blood vessels. Cells differentiated into early cardiomyocytes on membranes implanted in the left ventricles but not on those implanted in the aortas. Stem cell mobilization with GM-CSF led to more rapid tissue growth and differentiation. The GM-CSF effect on cell proliferation outlasted the treatment period by several weeks. Circulating stem cells contributed to the development of a fully differentiated tissue on membranes placed within the left ventricle or descending aorta under physiological conditions. Early cardiomyocyte generation was identified only on membranes positioned within the left ventricle.

Keywords: cardiac tissue engineering • myocardium • molecular biology • angiogenesis

Introduction

Cardiac remodelling processes that follow ischaemic damage or valvular and non-valvular cardiomyopathy are major sources of morbidity and mortality in industrialized countries. The heart itself has very limited potential for self-repair following such damage; therefore, therapeutic options designed to promote the repair of cardiac tissue are needed [1]. The potential therapeutic value of stem cells in cardiovascular medicine has attracted great attention in recent years. Various studies have reported that these cells can repair myocardial tissue after ischaemic damage by transdifferentiating into cardiomyocytes [2, 3] or by contributing to neoangiogenesis and scar tissue formation [4]. However, other groups have not detected meaningful rates of cellular differentiation using bone marrow-derived stem cells after myocardial infarction [5, 6]. Despite that early clinical trials have reported beneficial effects for stem cell transplantation following myocardial infarction [7], the potential for bone marrow-derived cells to adopt cardiomyocytic or endothelial phenotypes remains a matter of debate [8].

Recently, we demonstrated that a fully differentiated tissue grew on a septal occluder that had been implanted for 6 weeks to treat ventricular septum rupture secondary to conservatively treated myocardial infarction. The newly formed tissue consisted of inflammatory cells, fibroblasts, myofibroblasts, smooth muscle cells, endothelial cells and most interestingly, vascular structures. Because the occluder was in contact with only the largely devitalized septal scar tissue, we suggested that the cells comprising the tissue had not migrated per continuitatem but had derived from circulating stem cells [9, 10]. However, until now it has remained unclear as to what extent circulating stem cells differentiate or transdifferentiate in the absence of an acute pathological stimulus like myocardial infarction. Therefore, the aim of the present study

[#]These authors contributed equally.
*Correspondence to: Dr. Helge MÖLLMANN,
Kerckhoff Heart Center, Benekestrasse 2–8, 61231 Bad Nauheim, Germany.
Tel.: +49 6032 996 0
Fax: +49 6032 996 2827
E-mail: h.moellmann@kerckhoff-fgi.de

doi:10.1111/j.1582-4934.2009.00972.x

was to investigate the physiological differentiation and transdifferentiation potential of circulating cells in an *in vivo* model. Furthermore, we aimed to evaluate the hypothesis that circulating stem cells could build a differentiated tissue as was observed on the implanted septal occluder. For this purpose, we developed a pig model in which a membrane and scaffold were implanted within each the left ventricular cavum and the descending aorta, which served as an internal control. The membrane and scaffold were implanted so as to avoid direct contact of the membrane with the ventricular and vascular walls. This design allowed for the generation of tissue derived exclusively from circulating cells. To confirm this hypothesis, we increased the number of circulating stem cells by means of mobilization with the granulocyte macrophage colony-stimulating factor (GM-CSF). GM-CSF initiates the release of haematopoietic stem cells and other progenitor cells from bone marrow in the circulation typically leading to a significant increase of leucocytes [11].

Material and methods

Animal model

Sixty-four membrane/scaffold systems were implanted in the left ventricular cavums and the infra-renal aortas of 32 pigs and left for 3 days, or 2, 6 or 12 weeks (eight pigs per time-point). The membrane (Mersilene® band, Ethicon, Norderstedt, Germany) was mounted on a supporting scaffold using a 0.2 mm stainless steel wire. The scaffold consisted of a 10-cm-long piece of 5F coronary angiography catheter with both ends bent to form a curved shape (Fig. 1A). This special design allowed for delivery of the membrane/scaffold system to the left ventricular cavum (Fig. 1B) and the descending aorta (Fig. 1C) *via* a percutaneous approach. For this purpose, a 9F sheath (Cordis Corp., Warren, NJ, USA) was inserted in the right arteria femoralis and a 0.035 inch hydrophilic J-curved wire (Terumo, Eschborn, Germany) was placed in the left ventricle or the descending aorta. The membrane/scaffold systems were inserted under fluoroscopic and echocardiographic guidance over the wire using an 8F catheter and released at the desired position by carefully removing the wire (Fig. 1E). Only pigs in which adequate placement of the scaffold with a freely floating mersilene band (the membrane) could be unequivocally documented by echocardiography and fluoroscopy were used for the study. A loading dose of 300 mg clopidogrel was administered the day before implantation of the scaffolds. After implantation, pigs received clopidogrel (75 mg/day) and aspirin (100 mg/day). At the pre-specified intervals, animals were killed with 50 mmol potassium chloride under general anaesthesia. The hearts were excised quickly and the descending aortas were exposed. The scaffold systems were removed, snap-frozen in liquid nitrogen and stored at −80°C. All tissue sampling was completed within 4 min. of circulation being stopped.

An additional group of eight animals was treated similarly except that stem cell mobilization was performed for the first 7 days after implantation by subcutaneous administration of GM-CSF (GM-CSF REC SW, CatNo. PSC2011, Invitrogen, Karlsruhe, Germany; 10 μg/kg). In this group, the scaffold systems were removed after 6 weeks.

Cardiac function and scaffold placement were examined weekly by echocardiography (Aloka SSD-4000R, Meerbusch, Germany). Left ventricular diameter and ejection fraction were measured according to the method of Teichholz [12]. Animals in which scaffold implantation caused mitral or aortic valve regurgitation were replaced.

All animal experiments were performed according to the guidelines published by the Society for Laboratory Animal Science and were in compliance with the Guide for the Care and Use of Laboratory Animals (NIH Publication No. 85–23, revised 1996). The appropriate national authority (B2/167; Regierungspräsidium Darmstadt, Germany) approved the study protocol.

RNA isolation and quantitative real time-PCR

Total RNA was isolated (RNeasy Mini kit, Qiagen; Hilden, Germany) from left ventricular and aortic tissues and from tissue that had grown on the implanted membranes. After treatment with DNase-I (Turbo DNAfree, Ambion, Austin, TX, USA), cDNA was synthesized according to Superscript II reverse transcriptase (RT) protocol (Invitrogen) using 500 ng total RNA and 150 ng random nonamer oligonucleotides (NEB, Ipswich, CA, USA). Gene-specific RT-PCR primers were selected using FastPCR software (Institute of Biotechnology, University of Helsinki, Finland). Quantitative (q) RT-PCR was performed in a 25 μl reaction, 96-well format (1.0 μl cDNA [1:20]; 200 nM each primer; 1X IQ SYBR Green Super Mix [BioRad, Hercules, CA, USA]) using an iCycler RT-PCR system (BioRad). Samples were measured in triplicate, and a minimum of two independent experiments were performed. The relative amount of target mRNA normalized to 18S RNA was calculated as previously described [13].

Semi-thin sections and electron microscopy

Small tissue samples were embedded in Epon following routine protocols. Semi-thin sections (500 nm) were stained with toluidine blue and evaluated by light microscopy. Ultra-thin sections (70 nm) were stained with uranyl acetate and lead citrate and were viewed and photographed using a Philips CM 10 electron microscope (Philips GmbH, Hamburg, Germany).

Examination of scaffolds

To analyse a potential cell migration per continuitatem the scaffolds were embedded in a hydroxyethylmethacrylate polymer (Technovit 7100, Heraeus Kulzer GmbH & Co. KG, Germany) according to the manufacturer's instructions. After polymerization the samples were cut with a rotation microtome in slices of 200 μm (SP1600, Leica, Wetzlar, Germany) and stained with haematoxylin and eosin according to standard protocols.

Immunohistochemistry

Tissue samples were mounted with Tissue Tek (Sakura Finetec, Zoeterwoude, Netherlands) and cryosections were air-dried and fixed in paraformaldehyde. All sections were incubated for 1 hr at room temperature. Samples were treated with either Cy3-conjugated primary antibody or with primary antibody (Table 1) followed by biotinylated secondary antibody and fluoroisothiocyanate-linked streptavidin (Rockland, Gilbertsville, PA, USA). Nuclei were stained with Draq5 or DAPI (Invitrogen). For negative controls, secondary antibodies were omitted.

For immunohistological detection of GATA binding protein 4 (GATA4), the slides were incubated with a horseradish peroxidase-conjugated secondary

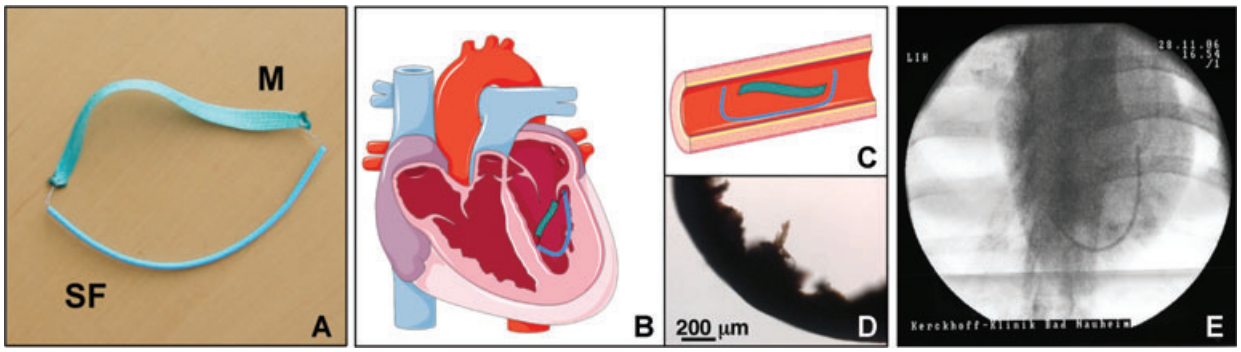

Fig. 1 (**A**) Membrane (M) and scaffold (SF). (**B**/**C**) Cartoon showing membrane/scaffold system placement within the left ventricle (**B**) and aorta (**C**). (**D**) Haematoxylin and eosin stained section of the scaffolds demonstrates the absence of invaded cells. (**E**) Position of the membrane/scaffold system in the left ventricle as documented by x-ray.

Table 1 Antibodies used

Antibody	Host	Dilution	Source
A-Smooth muscle actin clone IA4	Mouse	1:300	Sigma, Munich, Germany
Vimentin clone V9	Mouse	1:300	Sigma, Munich, Germany
SMemb	Mouse	1:1000	Abcam, Cambridge, UK
Connexin 43	Rabbit	1:100	Zymed, Munich, Germany
von Willebrand factor	Rabbit	1:500	Sigma, Munich, Germany
FGF2	Mouse	1:500	Peprotech, Hamburg, Germany
BS-1		1:500	Sigma, Munich, Germany
MF20	Mouse	1:200	DSHB, Iowa City, IA, USA
Nkx2.5	Goat	1:200	Santa Cruz, Santa Cruz, CA, USA
GATA4	Rabbit	1:100	Santa Cruz, Santa Cruz, CA, USA
c-kit	Rabbit	1:500	DAKO, Glostrup, Denmark
ki67 clone MIB 1	Mouse	1:50	DAKO, Glostrup, Denmark
CD3	Rat	1:50	Acris, Herford, Germany
CD14	Mouse	1:100	Cymbus Biotechnology, Southampton, UK
CD44	Rat	1:100	Calbiochem, Darmstadt, Germany
CD45	Mouse	1:100	Antibodies-online, Aachen, Germany
HMGB1	Mouse	1:50	Abnova, Heidelberg, Germany

antibody then treated with hydrogen peroxide and 3,3′-diaminobenzidine (DAB, Vector Labs, Burlingame, CA, USA). Sections were counterstained with haematoxylin. For ki67 staining, sections were pre-treated with citrate buffer solution (pH 6.0) in the microwave (600 W, 9 min.).

Used magnifications included 16×/100×/250× and 400×. The sections were viewed using a Leica TCS SP laser scanning confocal laser microscope (Leica) equipped with the following laser types: argon-uv (wave lengths of 351, 364 nm), argon/krypton (wave lengths of 488, 586, 647 nm) and helium/neon (wave lengths of 543 nm) lasers, appropriate filter blocks and a Silicon Graphics Octane workstation (Silicon Graphics, Sunnyvale, CA, USA) and three-dimensional multichannel image processing software (Bitplane, Zürich, Switzerland). Fibroblast growth factor-2 (FGF2) was quantified from specifically stained representative sections using Image J software version 1.35. Seven fields of vision, 40×, were randomly chosen. Contents were expressed in percentage of total tissue.

In situ hybridization

Digoxigenin (DIG)-labelled RNA-probes of cloned PCR products were synthesized by *in vitro* transcription using T7 and Sp6 polymerase according to the manufacturers' instructions (Promega Corp., Madison, WI, USA) and stored in aliquots at −20°C until use. Cryosections (12 µm) were fixed in 4% paraformaldehyde. After washing twice in phosphate buffered saline, a 2 min. proteinase K digest was performed (10 µg/ml; Carl Roth, Karlsruhe, Germany). Following post-fixation, the sections were acetylated. Hybridization was performed overnight using 0.5 ng probe/µl hybridization buffer in a wet chamber at 55°C. Probes were detected using an anti-DIG antibody (Roche Diagnostics GmbH, Mannheim, Germany). Slides were counterstained with eosin.

Statistical analysis

Data are expressed as means ± S.D. unless otherwise stated. Statistical comparisons between groups were performed by means of one-way ANOVA followed by the Bonferroni–Holmes test. *P*-values less than 0.05 were considered statistically significant. Analyses were performed using GraphPad Prism 4.02 (GraphPad Software Inc., La Jolla, CA, USA).

Results

Animal model

Implantation of the scaffolds was technically straightforward in most cases. In two pigs, the scaffolds could not be adequately

inserted in the left ventricular cavum and were washed into the aortic arch. One pig died after the scaffold perforated the left ventricular wall 6 days after implantation. In 10 pigs, the membrane was snared by the scaffold and therefore had direct contact with the left ventricle ($n = 3$) or the aorta ($n = 7$). These pigs were excluded from the study and replaced. Adequate placement was documented for the remainder of the scaffold systems. The scaffolds in the left ventricle did not lead to impaired valve function or injection fraction.

Tissue growth on scaffolds and membranes

An invasion of cells per continuitatem could be excluded given the lack of viable cells on the scaffolds (Fig. 1D). The tissue growth on both the aortic- and left ventricular-placed membranes was clearly time dependent. After 3 days, only scattered cells had colonized the membrane. The thickness of the newly developed tissue increased from 0.43 ± 0.06 mm after 2 weeks to 1.32 ± 0.18 mm after 6 weeks and 1.88 ± 0.22 mm after 12 weeks ($P < 0.05$; Fig. 2A–D). There was no difference in thickness between tissues grown in the aorta *versus* the left ventricle.

Differentiation potential

Until day 3, mainly $CD45^+$ leucocytes, $CD14^+$ monocytes and a few $CD3^+$ lymphocytes had invaded the membrane (Fig. 2B–G). The predominance of these inflammatory cells decreased over time. After day 14, $CD14^+$ monocytes were rare. The existence of spindle-like cells indicated a rather high degree of differentiation (Fig. 2C).

The inner part of the newly developed tissue contained large numbers of α-smooth muscle actin (α-SMA)$^+$ cells. Several of these cells were myofibroblasts, given the colocalization of α-SMA with vimentin (Fig. 3A) and their positive staining for embryonic smooth muscle myosin heavy chain (SMemb; Fig. 3B). The growing tissue was mainly defined by fibroblasts, as characterized by their typical shape and positive vimentin staining.

MF20 and Mef2c, as markers for any kind of myocyte, were found in membranes from both locations as early as 2 weeks after implantation (Fig. 3C–D). After 12 weeks, smooth muscle cells and fibroblasts were clearly aligned (Fig. 3E). Many fibroblasts showed high protein turnover as demonstrated by high amounts of rough endoplasmic reticulum (Fig. 3F). Dense bodies in the cytoplasm and focal adhesion points were observed in smooth muscle cells, while the extra cellular matrix showed collagen bunches (Fig. 3G).

Membranes removed after 6 or 12 weeks contained numerous BS-1^+ cells scattered in the inner parts of the tissue, indicating capillary growth (Fig. 4B). Integrity and functionality of the capillaries were indicated by cell–cell contacts (Fig. 4D) and tight junctions (Fig. 4E, F). Correspondingly, we found strong upregulation of basic FGF2 (Figs 4A and S1). The outermost cell layers, which were positive for vimentin, were also positive for von Willebrand factor (Fig. 4C). These endothelial cells appeared more densely packed in the membranes originating from the left ventricular cavum than in those originating from the aorta.

Cardiomyocytic cells

Detection of the myocyte markers MF20 and Mef2c prompted the hypothesis that cardiomyocyte differentiation had occurred. Therefore, we examined the membranes for markers of early and mature cardiomyocytes. Expression of the early cardiomyocyte marker GATA4 was documented by qRT-PCR and immunohistology in membranes that had been positioned within the left ventricular cavum for 6 weeks (Fig. 5A–C). The early cardiomyocyte markers Fog and Nkx2.5 were detected by qRT-PCR and immunohistochemistry, respectively (Fig. 5D). Furthermore, qRT-PCR verified BNP transcription in membranes that had been implanted in the left ventricle for 12 weeks (Fig. 5E). None of these early cardiomyocyte markers were detected on membranes that had been implanted in aortas. The mature cardiomyocyte markers troponin I, connexin 43 and sarcoplasmic reticulum ATPase (SERCA) 2a could not be detected on membranes originating from either location.

Contribution of stem cells

The potential contribution of stem cells to the observed tissue formation was investigated. We found a strong time-dependent increase in the expression of the stem cell markers CD34 and c-kit in tissues derived from both locations. There was no significant difference in mRNA abundance of either stem cell marker in membranes originating from the left ventricle *versus* the aorta (Fig. 6A, D). *In situ* hybridization showed that c-kit was expressed predominantly in the outer layers of the newly developed tissue. In the inner parts of the tissue, especially in those after 6 and 12 weeks, the vast majority of cells had differentiated and lost the stem cell marker c-kit (Fig. 6E, F).

Immunohistochemical analysis revealed the existence of $CD45^-/CD44^+$ mesenchymal stem cells (Fig. 7A). These cells showed a differentiation potential into fibroblasts (Fig. 7B) and endothelial cells (Fig. 7D–F), but not into smooth muscle cells (Fig. 7C).

The high-mobility group box 1 protein (HMGB1), which has been described to have stem cell attracting properties, was expressed strongly in left ventricular membranes after 2 and 6 weeks; the expression of HMGB1 in aortic membranes was comparatively weaker (Fig. 6B, C).

Endothelial progenitor cells, characterized by positive staining for CD133, were detected only sporadically.

Stem cell mobilization

Stem cell mobilization with GM-CSF was successful as demonstrated by a significant increase in leucocytes in the peripheral blood on day 8 ($14.9 \pm 1.1 \times 10^9$/l *versus* $29.1 \pm 2.3 \times 10^9$/l; $P < 0.05$; fluorescence-activated cell sorting (FACS) analysis). At

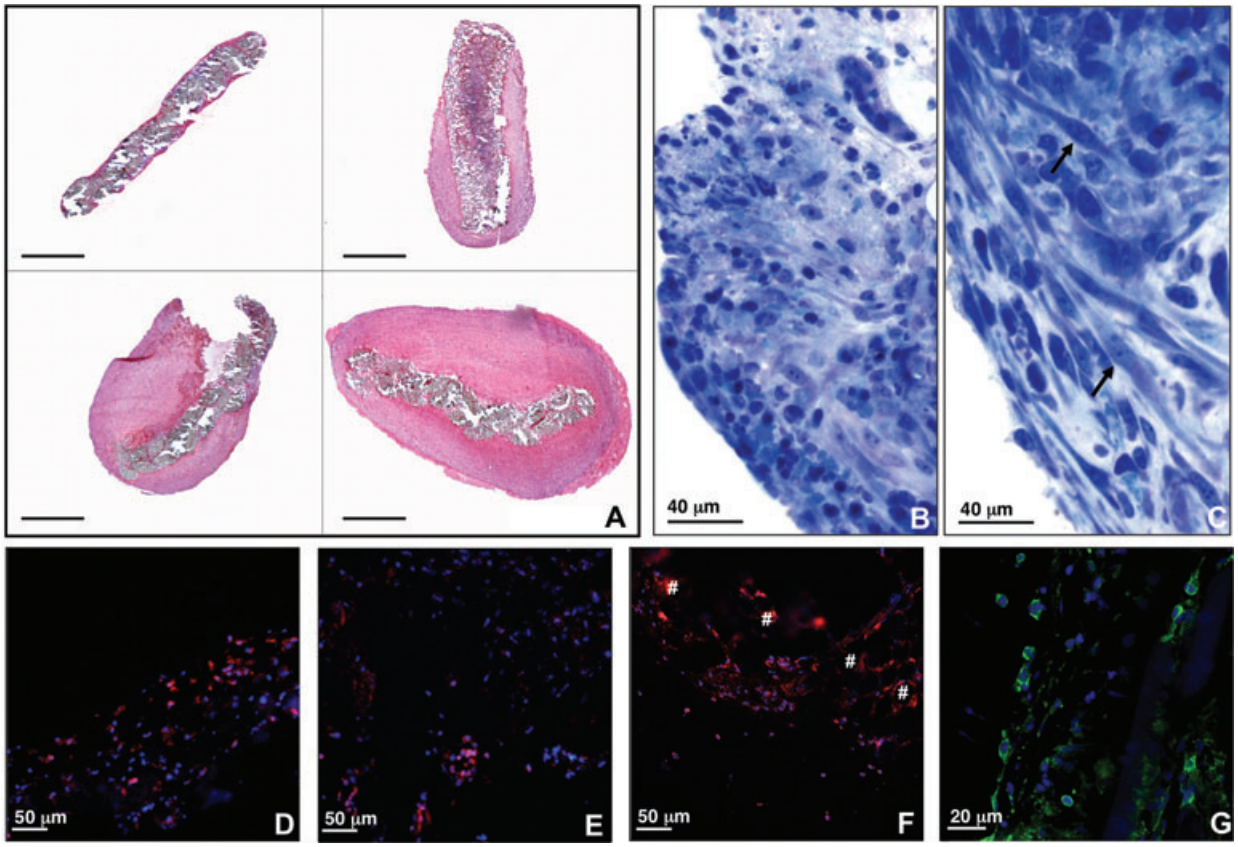

Fig. 2 (**A**) Haematoxylin and eosin staining of newly developed tissue on membranes after 3 days, 2 weeks, 6 weeks, 12 weeks. Scale bar = 1 mm. (**B**/**C**) Semi-thin sections of membranes. (**B**) After 3 days, membranes were coated (for the most part) with activated macrophages. (**C**) After 2 weeks, macrophages were decreased and spindle-like-cells (arrows) appeared, indicating a higher level of differentiation. (**D**/**E**) Specific staining for CD45 (red, nuclei blue) after 3 days (**D**) and 2 weeks (**E**). (**F**) Specific staining for CD14 (red, nuclei blue, 3 days). (**G**) Specific staining for CD3 (green, nuclei blue, 3 days).

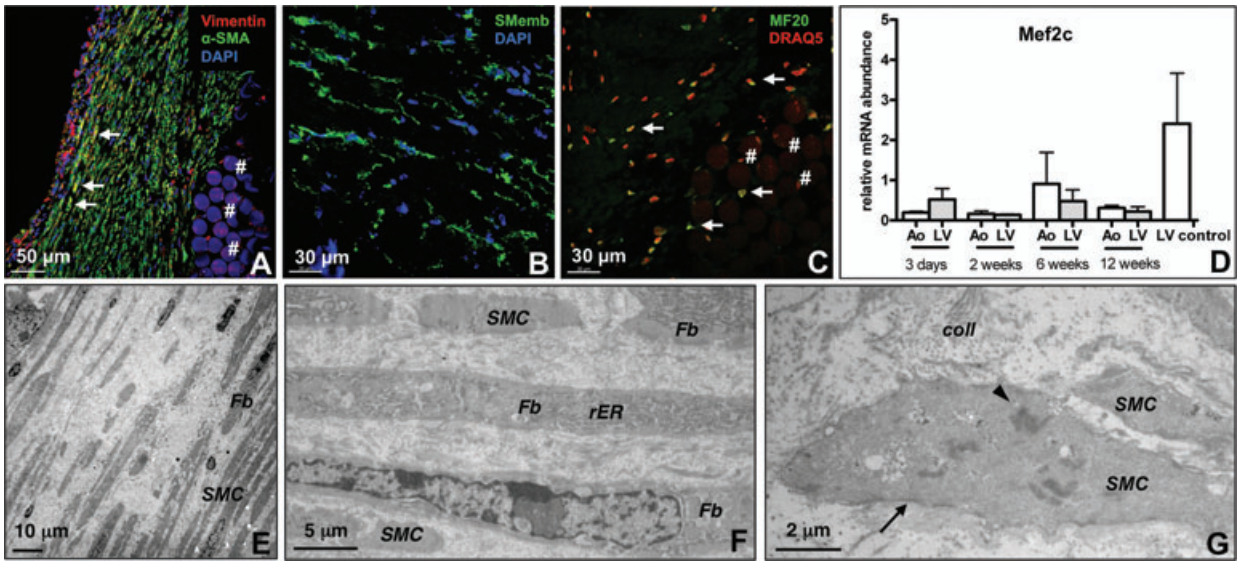

Fig. 3 (**A**) Fibroblasts are stained with vimentin (red), smooth muscle cells are stained with α-smooth muscle actin (α-SMA, green). Colocalization of vimentin and α-SMA is typical for myofibroblasts, which appear yellow (arrows). Nuclei are blue (#: implanted membrane). (**B**) Myofibroblasts specifically stained with anti-non-muscle myosin heavy chain b (SMemb; green); nuclei are blue. (**C**) Cells expressing myosin heavy chain were stained with MF20 (arrows, green), nuclei are red (#: implanted membrane). (**D**) Mef2c, a marker of muscle cells, was detected in aortic (Ao) and left ventricular membranes (qRT-PCR; $n = 8$ per time-point). (**E**) Electron microscopy image showing clear orientation of cells in the newly developed tissue after 12 weeks. (**F**) Electron microscopy image showing different types of differentiated cells after 6 weeks (SMC, smooth muscle cell; Fb, fibroblast; rER, rough endoplasmic reticulum). (**G**) Electron microscopy image showing SMCs and organized collagen fibres (coll). Intracellular dense bodies (arrowhead) indicate terminal differentiation and contractile function of SMCs. Focal adhesion points (arrow) hallmark cellular interaction with the extracellular matrix, implying functional organization.

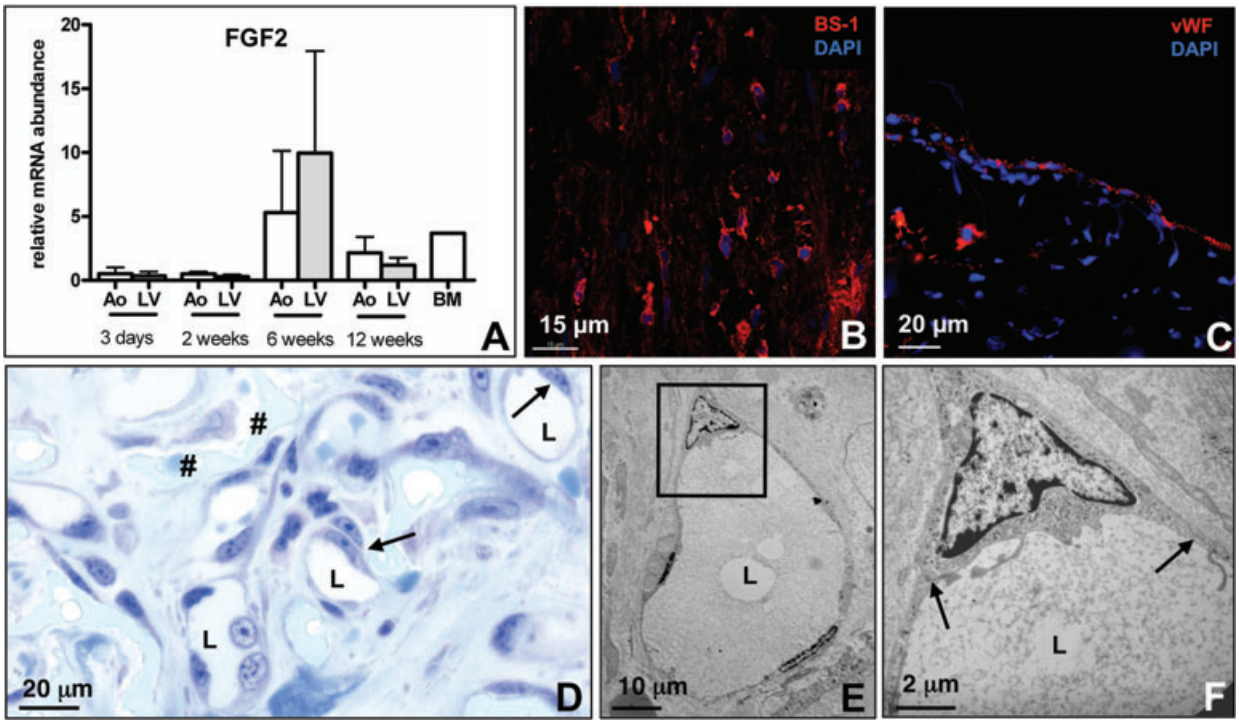

Fig. 4 (**A**) Time-dependent expression profile of FGF2 (qRT-PCR; $n = 8$ per time-point); peak expression occurred after 6 weeks (BM, bone marrow). (**B**) BS-1 staining of endothelial cells. (**C**) Localization of endothelial cells in the outer cell layer (anti-vWF). (**D**) Toluidine blue staining of semi-thin sections demonstrates capillaries in the developed tissue. Endothelial cells are indicated by arrows (L, capillary lumen; #, implanted membrane). (**E**) Electron microscopy of a capillary structure. (**F**) Higher magnification of image in (**E**) shows cell–cell contacts of endothelial cells (arrows) surrounding the lumen.

6 weeks after implantation, the abundance of c-kit mRNA was three times greater in animals treated with GM-CSF than in non-treated animals (Fig. 8D).

At 6 weeks, tissue formation was significantly more robust in animals that had received stem cell mobilization than in non-treated animals. In animals treated with GM-CSF, the extent of tissue formation after 6 weeks was comparable to that in non-treated animals after 12 weeks (GM-CSF 6 weeks: 1.85 ± 0.14 mm; no treatment 6 weeks: 1.32 ± 0.18 mm, $P < 0.05$; no treatment 12 weeks: 1.88 ± 0.22 mm; not significant). Correspondingly, the rate of cell proliferation, as measured by staining for the proliferation marker ki67, was significantly higher in membranes originating from pigs treated with GM-CSF than in non-treated control animals (11.46 ± 5.3% *versus* 22.2 ± 8.1%, $P < 0.05$; Fig. 8A–C).

Similar to the results for c-kit, stem cell mobilization led to a significant 4-fold greater abundance in GATA4 mRNA (an early cardiomyocyte marker) at 6 weeks (Fig. 8E).

Discussion

The aim of our study was to examine the physiological differentiation and transdifferentiation potential of circulating stem cells in the absence of ischaemic or other myocardial damage in an *in vivo*

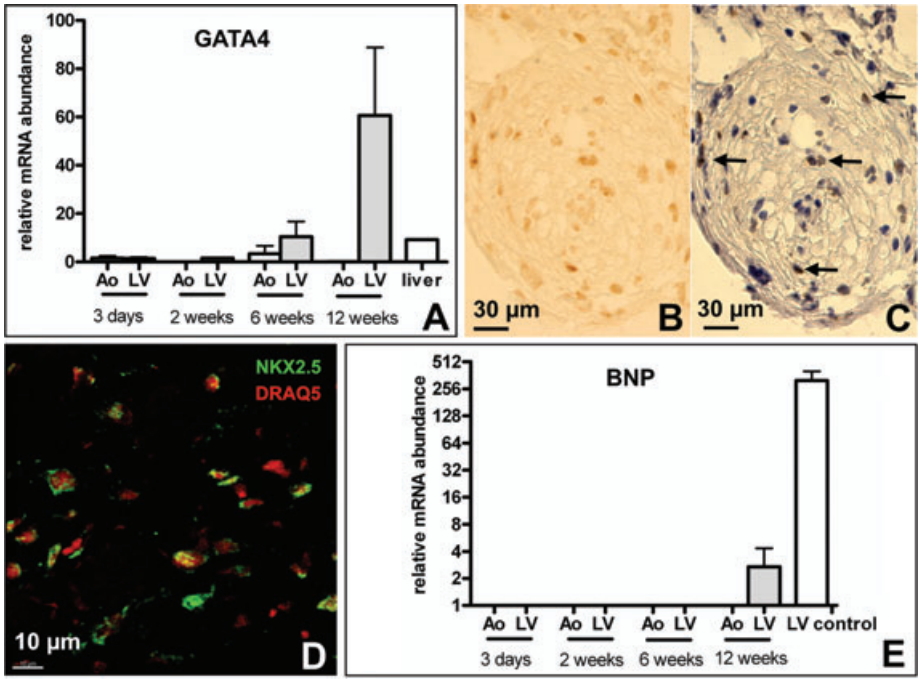

Fig. 5 (**A**) The early cardiomyocyte marker GATA4 was detected only in the membranes implanted in the left ventricle and not in those implanted in the aorta (qRT-PCR; $n = 8$ per time-point). (**B–C**) GATA4 staining with DAB (brown, arrows); nuclei are counterstained with haemalaun. (**D**) Early forms of cardiomyocytes expressing Nkx2.5 (green); nuclei are red. (**E**) BNP expression was evident in membranes from the left ventricles after 12 weeks, indicating further differentiation of early cardiomyocytes (qRT-PCR; $n = 8$ per time-point).

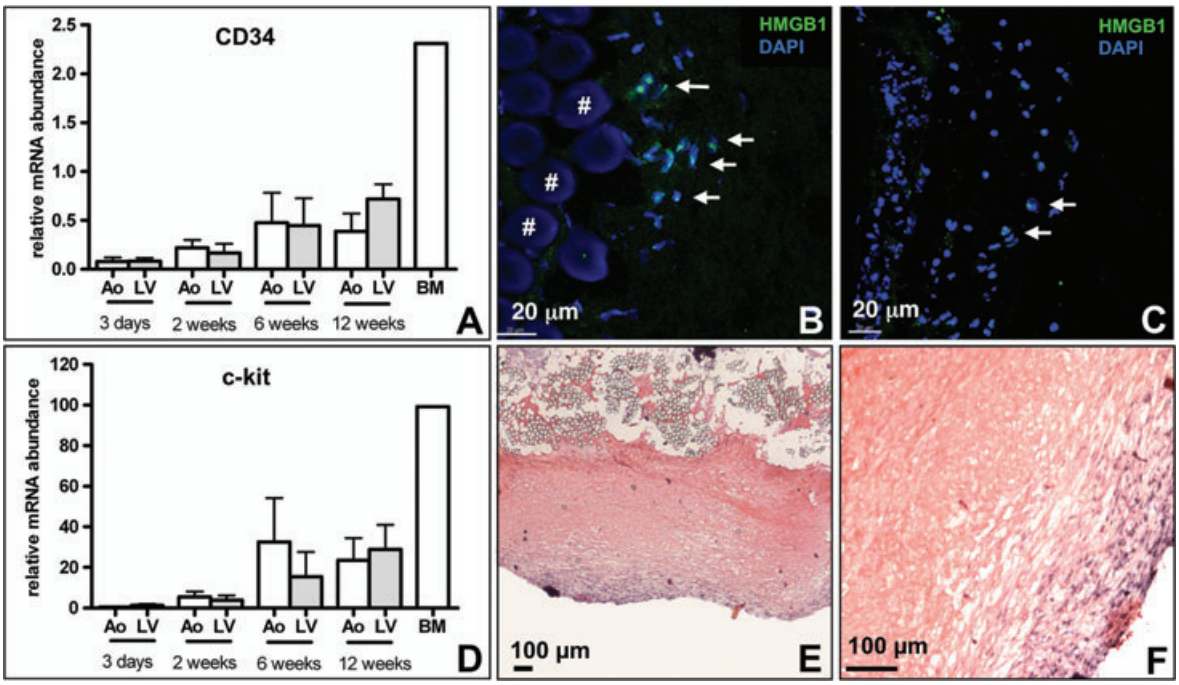

Fig. 6 (**A**) qRT-PCR shows time-dependent expression of the stem cell marker CD34 on membranes from both compartments, indicating the contribution of stem cells to tissue formation ($n = 8$ per time-point). (**B–C**) Specific staining for HMGB1 (green, arrows), a potential stem cell-attracting factor. More cells are positive for HMGB1 in left ventricular membranes (**B**) than in aortic membranes (**C**). Nuclei are blue. #, implanted membrane. (**D**) Transcription analysis shows time-dependent expression of the stem cell marker c-kit (qRT-PCR; $n = 8$ per time-point). (**E–F**) In situ hybridization of c-kit. The outer layers show distinct and specific staining for c-kit (blue), whereas the inner layers have already differentiated and ceased to express c-kit. BM, bone marrow.

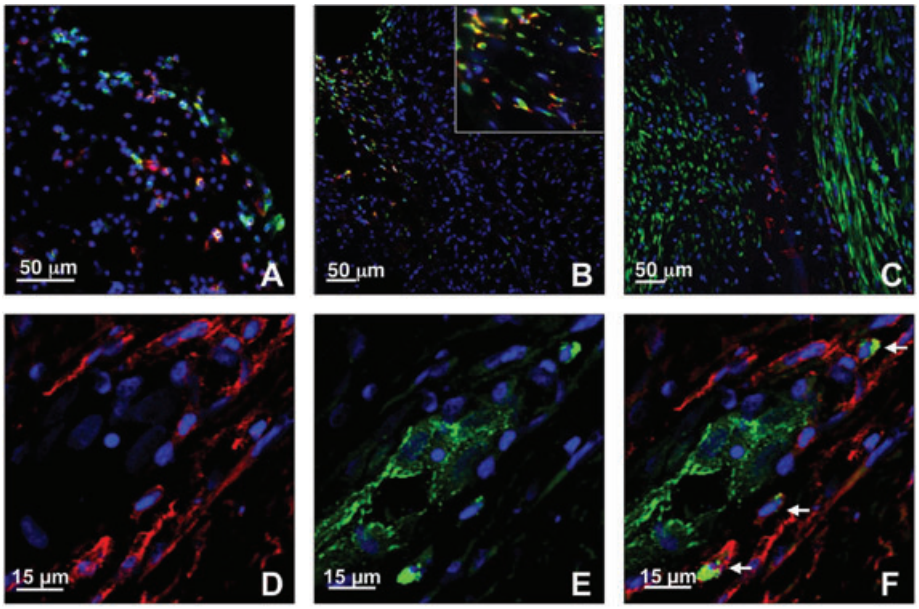

Fig. 7 (**A**) Co-staining for CD44 (red) and CD45 (green), nuclei are blue. $CD44^+/CD45^+$ cells are lymphocytes/monocytes, $CD44^+/CD45^-$ cells are mesenchymal stem cells, $CD44^-/CD45^+$ cells are leucocytes. (**B**) Co-staining for CD44 (red) and vimentin (green), nuclei are blue. Colocalization demonstrates mesenchymal stem cell derived fibroblasts. (**C**) Co-staining for CD44 (red) and alpha smooth muscle actin (green), nuclei are blue. (**D**–**F**) Co-staining for CD44 (red) and the endothelial cell marker CD31 (green), nuclei are blue. Colocalization (arrow) demonstrates mesenchymal stem cell derived endothelial cells.

model. The main finding was that circulating cells were capable of building a fully differentiated tissue on intraventricular and intravascular membranes. This tissue was composed of fibroblasts, myofibroblasts, smooth muscle cells, capillaries and on membranes implanted in the left ventricle, early forms of cardiomyocytes.

The newly developed animal model was suitable for testing our initial hypothesis. The design of our investigational device, with the membrane mounted to a scaffold using a stainless steel wire, minimized the potential for cell invasion from surrounding tissues per continuitatem. Based on our results, we postulate that circulating cells initialized the observed tissue generation.

The tissue growth on membranes from both the aorta and the left ventricle did not conform to the traditional model of a foreign body reaction in which mainly macrophages fuse to form foreign body giant cells during the first 2–4 weeks [14, 15]. On the contrary, macrophages were only present at very early stages and disappeared progressively until day 14 without having built multinuclear foreign body giant cells. Instead, a sponge-like differentiated tissue consisting of smooth muscle cells, myofibroblasts and fibroblasts surrounded the membranes. The outermost cell layers were positive for the classical endothelial cell markers BS-1, von Willebrand factor and for vimentin, characterizing these cells as a migrating subtype of endothelial cell [16]. The strong expression of FGF2 in the newly developed tissue suggested that neoangiogenesis might be occurring, and numerous endothelial cells were found in capillaries within the newly developed tissue. It is known that during tissue generating processes such as wound healing or tumour development, heparin sulphate-degrading enzymes activate FGF2, thus mediating the formation of new blood vessels [17, 18].

A major finding of the present study was the existence of cardiomyocyte precursors in left ventricular membranes beginning at 6 weeks after implantation and the absence of these cells in membranes from the aorta even after 12 weeks. These early cardiomyocytes were characterized using different methods and several different targets, making misinterpretation unlikely. GATA4, Nkx2.5 and Fog were used as markers of early cardiomyocyte differentiation. All of these markers have been described to be unequivocally specific for the cardiomyocytic lineage [19–21]. Furthermore, the abundance of GATA4 mRNA showed a time-dependent increase. The detection of BNP expression by qRT-PCR in membranes implanted in the left ventricle for 12 weeks further supports cardiomyocyte differentiation. BNP is known to be expressed not only by mature cardiomyocytes but also by intermediate forms, in which it is regulated by GATA4 [22, 23].

Despite intense searching, we did not find evidence of mature cardiomyocytes. Neither SERCA2a, troponin I, nor connexin 43 could be detected. These findings clearly indicate that the observed early cardiomyocyte markers were not the result of contamination by mature cardiomyocytes through direct contact with left ventricular structures. It is possible the early and intermediate cardiomyocytes (demonstrated by GATA4, Nkx2.5 and Fog after 6 weeks and BNP after 12 weeks) could have developed into mature cardiomyocytes at later time-points.

Whereas the cardiac-specific markers GATA4, Nkx2.5, Fog and BNP could only be detected in membranes derived from the left ventricular scaffolds, MF20 and Mef2c, as markers of both cardiac and skeletal muscle, were also present in membranes implanted in aortas [24, 25]. The reason for this striking difference is not clear. It is possible that differences in blood pressure between the left ventricle and the aorta, with a higher d_p/d_t in the left ventricular cavum, the more pronounced shear stress in the left ventricle *versus* the laminar flow in the aorta, or the direction of the membrane to the blood flow contributed to the differences in tissue development between the two compartments. It has been shown under *in vitro* conditions that oscillating pressure is a prerequisite for

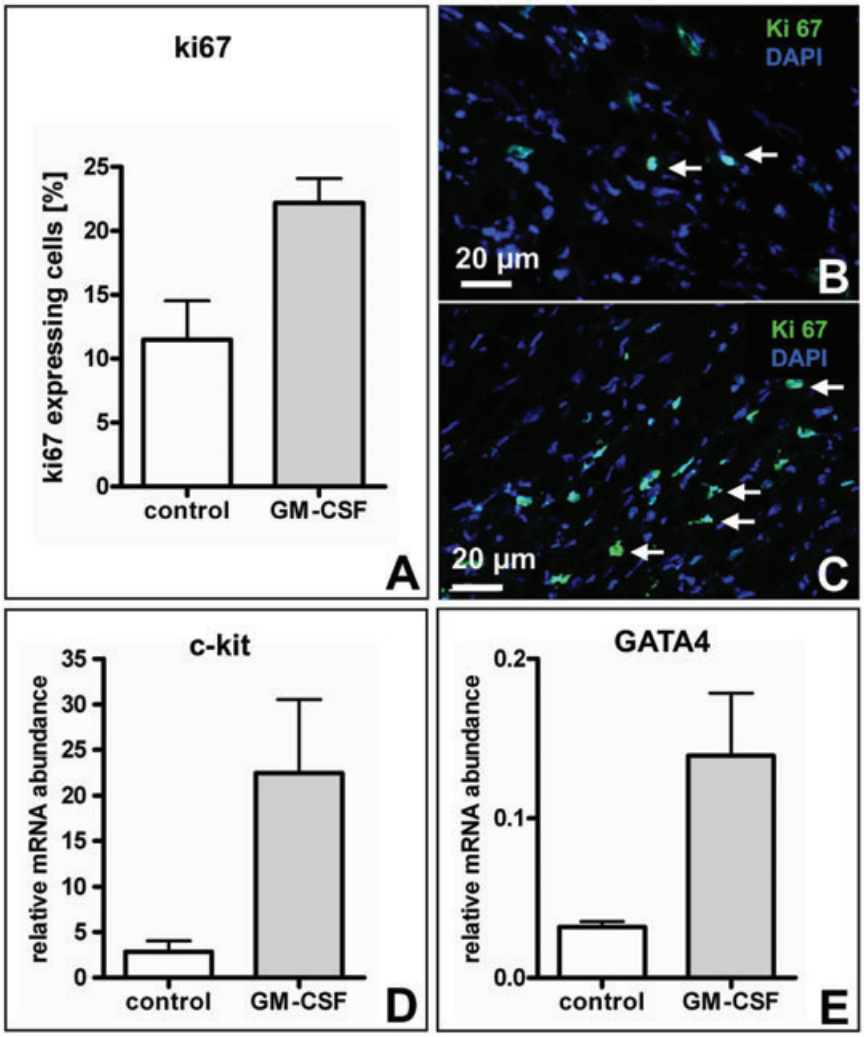

Fig. 8 (**A**) Mobilization of stem cells with GM-CSF led to a significant increase in expression of the proliferation marker ki67 after 6 weeks. (**B**, **C**) Tissues from non-treated animals (**B**) showed significantly fewer numbers of $ki67^{+}$ cells (green, arrows) than did tissues from animals treated with GM-CSF (**C**); nuclei are blue. (**D**) qRT-PCR shows a significant increase in the abundance of c-kit mRNA in tissues from GM-CSF-treated animals relative to non-treated animals (after 6 weeks, $n = 6$). (**E**) Stem cell mobilization led to a significant increase in the abundance of GATA4 mRNA after 6 weeks ($n = 6$).

the transdifferentiation of mesenchymal stem cells into early cardiomyocytes [26]. It is also possible that differences in the cytokine milieu contributed to the compartment-specific cell differentiation and tissue development patterns; however, given that blood leaving the left ventricular cavum reaches the descending aorta only seconds later, this explanation is rather unlikely. Further research is necessary to clarify this finding.

Because the membranes were implanted so as to avoid contact with the left ventricular and aortic walls, it is likely that the observed tissue generating processes originated from circulating stem cells as opposed to per continuitatem from surrounding tissues. It is known that during foreign body reactions provoked by procedures similar to those used herein there is substantial recruitment of haematopoietic stem cells. These cells eventually transdifferentiate into myofibroblasts [27] and other cell types [28]. Further support for the hypothesis of stem cell-derived tissue growth was provided by the time-dependent increase in the stem cell markers CD34 and c-kit. We also demonstrated profound expression of HMGB1, especially at early time-points and in the left ventricular membranes. This protein has been largely characterized for its role in inflammation since it is released into the extracellular space by activated macrophages [29]. However, it was recently demonstrated that HMGB1 also contributes to post-myocardial infarction repair by recruiting stem cells to the site of injury [30, 31] and by stimulating growth factor, cytokine and chemokine release by cardiac fibroblasts [32]. These data suggest that HMGB1 could have initialized stem cell attraction and tissue differentiation in our experimental system.

In order to functionally investigate the role of stem cells during tissue generation, we used GM-CSF to mobilize stem cells during the first week after scaffold/membrane implantation. Stem cell mobilization led to significantly faster tissue generation in treated animals relative to non-treated animals. This accelerated tissue growth outlasted the actual interval of stem cell mobilization by far: the rate of cell proliferation as determined by ki67 staining remained significantly higher in treated animals even 5 weeks after

termination of GM-CSF treatment. These data are in good correspondence with results of other groups, which documented an increase of neointimal overgrowth in stented vessels after stem cell mobilization [33]. Further research is necessary in order to clarify whether the observed accelerated tissue generation has primarily been caused by the increased number of circulating cells or whether direct effects of GM-CSF on cardiac cells may also play a role. However, the latter seems questionable, given that GM-CSF effects persisted 5 weeks after termination of treatment.

The fact that circulating cells are capable to induce growth of a differentiated tissue including cardiomyocyte generation in membranes placed inside the left ventricle potentially offers therapeutical application in hearts being at risk to develop aneurysms after large myocardial infarctions. Attempts to address this problem from the epicardial side of the ventricular wall showed were hampered by an impaired engraftment of the cells [34]. Therefore, an intraventricular access as chosen in our model may have the advantage of direct contact to circulating (stem) cells, making contact to other viable structures unnecessary.

Limitations

Our experimental setup did not allow for a traditional control group. Placement of a scaffold and membrane in places other than the circulatory system is associated with a strong foreign body reaction, resulting in rapid encapsulation of the implanted material. Furthermore, our precondition that the membrane must not have contact with the surrounding structures in order to avoid migration of any cells per continuitatem would have been impossible to meet in a control group.

Although our model excluded an invasion of cells per continuitatem as far as possible the origin of the documented c-kit expressing cells (circulating stem cells or cardiac stem cells) remains to a certain degree unclarified.

The functional relevance of the cardiomyocytogenic differentiation cannot be determined using our scaffold/membrane-model but deserves further evaluation.

Conclusions

In conclusion, we demonstrated that circulating stem cells prompted the development of a fully differentiated tissue, which included vascular structures, on membranes placed within the left ventricle and the descending aorta under physiological conditions. Interestingly, the development of early forms of cardiomyocytes was restricted to membranes implanted in the left ventricle.

Acknowledgements

This work was generously supported by the Kerckhoff Foundation, the Max-Planck-Gesellschaft (GFR-Projekt), and the Excellence Cluster – Cardio-Pulmonary system (ECCPS).

Supporting Information

Additional Supporting Information may be found in the online version of this article:

Fig. S1 Representative sections with specific labelling for FGF2 in left ventricular membranes demonstrate a time-dependent increase. (**A**) 3 days; (**B**) 2 weeks; (**C**) 6 weeks; (**D**) 12 weeks; (**E**) 6 weeks + GM-CSF treatment; (**F**) quantification of FGF2-amount. Quantification was performed in seven fields of vision (magnification 40×; $n = 6$ for each time-point). Stem cell mobilization leads to a strong increase of FGF2 in comparison to non-treated animals.

Please note: Wiley-Blackwell are not responsible for the content or functionality of any supporting materials supplied by the authors. Any queries (other than missing material) should be directed to the corresponding author for the article.

References

1. **Passier R, van Laake LW, Mummery CL.** Stem-cell-based therapy and lessons from the heart. *Nature*. 2008; 453: 322–9.
2. **Orlic D, Kajstura J, Chimenti S, *et al.*** Bone marrow cells regenerate infarcted myocardium. *Nature*. 2001; 410: 701–5.
3. **Orlic D, Kajstura J, Chimenti S, *et al.*** Mobilized bone marrow cells repair the infarcted heart, improving function and survival. *Proc Natl Acad Sci USA*. 2001; 98: 10344–9.
4. **Mollmann H, Nef HM, Kostin S, *et al.*** Bone marrow-derived cells contribute to infarct remodelling. *Cardiovasc Res*. 2006; 71: 661–71.
5. **Balsam LB, Wagers AJ, Christensen JL, *et al.*** Haematopoietic stem cells adopt mature haematopoietic fates in ischaemic myocardium. *Nature*. 2004; 428: 668–73.
6. **Murry CE, Soonpaa MH, Reinecke H, *et al.*** Haematopoietic stem cells do not transdifferentiate into cardiac myocytes in myocardial infarcts. *Nature*. 2004; 428: 664–8.
7. **Schachinger V, Erbs S, Elsasser A, *et al.*** Intracoronary bone marrow-derived progenitor cells in acute myocardial infarction. *N Engl J Med*. 2006; 355: 1210–21.
8. **Sussman MA, Murry CE.** Bones of contention: marrow-derived cells in myocardial regeneration. *J Mol Cell Cardiol*. 2008; 44: 950–3.
9. **Elsasser A, Mollmann H, Nef H, *et al.*** Transcatheter closure of a ruptured

ventricular septum after myocardial infarction using a venous approach. *Z Kardiol*. 2005; 94: 684–9.

10. **Mollmann H, Nef HM, Kostin S, *et al.*** Images in cardiovascular medicine. Natural tissue engineering inside a ventricular septum defect occluder. *Circulation*. 2006; 113: e718–9.
11. **Kessinger A, Sharp JG.** Mobilization of blood stem cells. *Stem Cells*. 1998; 16: 139–43.
12. **Schiller NB, Shah PM, Crawford M, *et al.*** Recommendations for quantitation of the left ventricle by two-dimensional echocardiography. American Society of Echocardiography Committee on Standards, Subcommittee on Quantitation of Two-Dimensional Echocardiograms. *J Am Soc Echocardiogr*. 1989; 2: 358–67.
13. **Pfaffl MW.** A new mathematical model for relative quantification in real-time RT-PCR. *Nucleic Acids Res*. 2001; 29: 2002–7.
14. **van Amerongen MJ, Harmsen MC, Petersen AH, *et al.*** The enzymatic degradation of scaffolds and their replacement by vascularized extracellular matrix in the murine myocardium. *Biomaterials*. 2006; 27: 2247–57.
15. **Anderson JM, Rodriguez A, Chang DT.** Foreign body reaction to biomaterials. *Semin Immunol*. 2008; 20: 86–100.
16. **Obermeyer N, Janson N, Bergmann J, *et al.*** Proteome analysis of migrating versus nonmigrating rat heart endothelial cells reveals distinct expression patterns. *Endothelium*. 2003; 10: 167–78.
17. **Ornitz DM, Itoh N.** Fibroblast growth factors. *Genome Biol*. 2001; 2: REVIEWS3005.
18. **Amann K, Faulhaber J, Campean V, *et al.*** Impaired myocardial capillarogenesis and increased adaptive capillary growth in FGF2-deficient mice. *Lab Invest*. 2006; 86: 45–53.
19. **Durocher D, Charron F, Warren R, *et al.*** The cardiac transcription factors Nkx2–5 and GATA-4 are mutual cofactors. *EMBO J*. 1997; 16: 5687–96.
20. **Svensson EC, Tufts RL, Polk CE, *et al.*** Molecular cloning of FOG-2: a modulator of transcription factor GATA-4 in cardiomyocytes. *Proc Natl Acad Sci USA*. 1999; 96: 956–61.
21. **Molkentin JD, Kalvakolanu DV, Markham BE.** Transcription factor GATA-4 regulates cardiac muscle-specific expression of the alpha-myosin heavy-chain gene. *Mol Cell Biol*. 1994; 14: 4947–57.
22. **Grepin C, Dagnino L, Robitaille L, *et al.*** A hormone-encoding gene identifies a pathway for cardiac but not skeletal muscle gene transcription. *Mol Cell Biol*. 1994; 14: 3115–29.
23. **Thuerauf DJ, Hanford DS, Glembotski CC.** Regulation of rat brain natriuretic peptide transcription. A potential role for GATA-related transcription factors in myocardial cell gene expression. *J Biol Chem*. 1994; 269: 17772–5.
24. **Allegra S, Li JY, Saez JM, Langlois D.** Terminal differentiation of Sol 8 myoblasts is retarded by a transforming growth factor-beta autocrine regulatory loop. *Biochem J*. 2004; 381: 429–36.
25. **Krainc D, Haas M, Ward DC, *et al.*** Assignment of human myocyte-specific enhancer binding factor 2C (hMEF2C) to human chromosome 5q14 and evidence that MEF2C is evolutionarily conserved. *Genomics*. 1995; 29: 809–11.
26. **Chang SA, Lee EJ, Kang HJ, *et al.*** Impact of myocardial infarct proteins and oscillating pressure on the differentiation of mesenchymal stem cells: effect of acute myocardial infarction on stem cell differentiation. *Stem Cells*. 2008; 26: 1901–12.
27. **Campbell JH, Efendy JL, Han C, *et al.*** Haemopoietic origin of myofibroblasts formed in the peritoneal cavity in response to a foreign body. *J Vasc Res*. 2000; 37: 364–71.
28. **Vranken I, De Visscher G, Lebacq A, *et al.*** The recruitment of primitive Lin(-) Sca-1(+), CD34(+), c-kit(+) and CD271(+) cells during the early intraperitoneal foreign body reaction. *Biomaterials*. 2008; 29: 797–808.
29. **Wang H, Yang H, Tracey KJ.** Extracellular role of HMGB1 in inflammation and sepsis. *J Intern Med*. 2004; 255: 320–31.
30. **Limana F, Germani A, Zacheo A, *et al.*** Exogenous high-mobility group box 1 protein induces myocardial regeneration after infarction *via* enhanced cardiac C-kit+ cell proliferation and differentiation. *Circ Res*. 2005; 97: e73–83.
31. **Germani A, Limana F, Capogrossi MC.** Pivotal advances: high-mobility group box 1 protein–a cytokine with a role in cardiac repair. *J Leukoc Biol*. 2007; 81: 41–5.
32. **Rossini A, Zacheo A, Mocini D, *et al.*** HMGB1-stimulated human primary cardiac fibroblasts exert a paracrine action on human and murine cardiac stem cells. *J Mol Cell Cardiol*. 2008; 44: 683–93.
33. **Cho HJ, Kim TY, Park KW, *et al.*** The effect of stem cell mobilization by granulocyte-colony stimulating factor on neointimal hyperplasia and endothelial healing after vascular injury with bare-metal versus paclitaxel-eluting stents. *J Am Coll Cardiol*. 2006; 48: 366–74.
34. **Derval N, Barandon L, Dufourcq P, *et al.*** Epicardial deposition of endothelial progenitor and mesenchymal stem cells in a coated muscle patch after myocardial infarction in a murine model. *Eur J Cardiothorac Surg*. 2008; 34: 248–54.